ELSEVIER

0309-1708(95)00020-4

*Advances in Water Resources* **18** (1995) 25–38

0309-1708/95/$09.50

# Robust numerical methods for saturated–unsaturated flow with dry initial conditions in heterogeneous media

**P. A. Forsyth**

*Department of Computer Science, University of Waterloo, Waterloo, Ontario, Canada, N2L 3G1*

**Y. S. Wu**

*HydroGeoLogic, Herndon, Virginia 22070, USA*

&

**K. Pruess**

*Earth Sciences Division, Lawrence Berkeley Laboratory, University of California, Berkeley, California 94720, USA*

(Received 18 July 1994; accepted 6 October 1994)

A robust numerical method for saturated–unsaturated flow is developed which uses a monotone discretization and variable substitution. This method is compared to a conventional formulation and to a two phase (active air phase) model. On some published test examples of infiltration into dry media, the variable substitution method shows an order of magnitude improvement (in terms of nonlinear iterations) compared to the conventional pressure based method. One, two and three dimensional computations using both finite element and finite volume discretizations are presented.

*Key words:* saturated–unsaturated flow, dry conditions, variable substitution, monotonicity.

## 1 INTRODUCTION

Analysis of waste cover designs[18] and evaluation of low level nuclear waste disposal facilities[25,29] requires solution of unsaturated–saturated flow models. Since there is a great deal of uncertainty regarding the physical parameters in these models, Monte Carlo methods are often used to obtain expected and worst case estimates of infiltration through these waste sites. This means that simulations must be carried out many times for each design in order to obtain a statistically reasonable sample size. In certain cases, full three dimensional models are required to fully capture the site geometry. Consequently, the basic flow model must be very efficient and robust.

In order to minimize infiltration, many waste sites have been situated in arid regions. As a result, these sites have large unsaturated zones, which are initially very dry. The various capping technologies currently under evaluation[18] utilize capillary or clay barriers to divert moisture away from the buried waste. Other designs[29] use a combination of capillary barriers and low permeability barriers. Multiple capillary barriers have also been proposed.[37] This means that simulations of these sites must be able to handle highly heterogeneous systems.

It is well known that numerical simulation of water infiltration into dry soils is a very difficult numerical problem when the usual constant air phase pressure assumption is invoked.[5,19,23,28,30,36,38] For practical purposes, it is desirable to be able to model flow in both the saturated and unsaturated zones, which rules out a pure water content based formulation.

A head or pressure based method can be used for both saturated and unsaturated flow, but under dry initial conditions, the capillary pressure curve is an extremely nonlinear function. This causes convergence difficulties for the nonlinear iteration unless very small timesteps are used.[7,23,36] The timesteps required for convergence

may be orders of magnitude smaller than is required for reasonable time discretization errors.[30,36]

Recently, a comparative study of various saturated–unsaturated flow simulators was carried using a two dimensional test problem.[36] This problem was inspired by the Las Cruces Trench field experiment. It was noted that numerical simulation of this experiment proved to be very difficult. Existing simulators required an inordinate number of Newton iterations and/or time-steps. The model for the field experiment was abstracted to produce a simple data set which still captured the numerical difficulties.[36] All of the standard simulators used a very large number of nonlinear iterations to solve this problem. However, rather surprisingly, use of a true two phase (non-constant air phase pressure) flow model for this problem proved to be very efficient.[36]

The objective of this article is to develop a robust and general purpose method for simulating saturated–unsaturated flow using the constant air phase pressure approximation. Desirable characteristics of a robust numerical method include the following:

- The discretization should be mass conservative regardless of timestep or mesh size. The importance of mass conservation has been noted in Celia *et al.*[5]
- The technique for solving the nonlinear discrete equations should be efficient for very dry conditions. For regions where the water saturation is unity, the formulation should be as efficient as a standard method.
- Heterogeneous media having variable permeability and capillary pressure, and discontinuous absolute permeabilities, should be handled in a natural and efficient manner. In particular, heterogeneities should cause no new discontinuities (as a result of the numerical formulation) in the equation coefficients.
- The discretization should be monotone. The importance of monotonicity was emphasized in Celia *et al.*[5] and Forsyth.[11,12]

In the remainder of this paper, we will present a numerical formulation which satisfies these criteria for robustness. Numerical results will be presented for the two dimensional test problem[36] and other published problems which are considered to be examples of difficult test cases.[23] Computational simulations will also be carried out for some three dimensional examples. The two dimensional computations will be compared to simulations which use a true two phase (non-constant air phase pressure) formulation. Test examples having up to 50 000 nodes will be shown. All computations were carried out on workstations using either finite element or finite volume spatial discretizations.

## 2 FORMULATION

To avoid repetition, the formulation will be given for a two phase (active air phase) model of saturated–unsaturated flow. The constant air phase pressure approximation is a special case of this formulation.

The two phases considered here are water ($w$) and air ($a$). Conservation of phase $l$ then implies

$$\frac{\partial}{\partial t}(\phi S_l \rho_l) = \nabla \cdot (\rho_l \mathbf{V}_l) + q_l \tag{1}$$

where the velocity of each phase $l$ is given by

$$\mathbf{V}_l = -\mathbf{K} \cdot \lambda_l (\nabla P_l - \rho_l g \nabla D) \tag{2}$$

and where

$$\begin{aligned} S_l &= \text{saturation of phase } l \\ P_l &= \text{pressure of phase } l \\ \rho_l &= \text{mass density of phase } l \\ \mathbf{K} &= \text{absolute permeability tensor} \\ \lambda_l &= k_{rl}/\mu_l \\ \mu_l &= \text{viscosity of phase } l \\ k_{rl} &= \text{relative permeability of phase } l \\ D &= \text{depth} \\ g &= \text{gravitational acceleration} \\ q_l &= \text{source/sink term for phase } l \end{aligned} \tag{3}$$

The phase pressures are related by the capillary pressure $P_{caw}$

$$P_a = P_w + P_{caw}(S_w) \tag{4}$$

For true two phase formulations (non-constant air phase pressure) we have

$$S_w + S_a = 1 \tag{5}$$

The phase densities and porosity are given by

$$\begin{aligned} \rho_w &= \rho_{w0}(1 + c_w(P_w - P_{w0})) \\ \rho_a &= \rho_{a0} P_a / P_{a0} \\ \phi &= \phi_0 (1 + c_m (P_w - P_{w0})) \end{aligned} \tag{6}$$

where $\rho_{w0}$, $\rho_{a0}$ are the densities at pressures $P_{w0}$ and $P_{a0}$, $c_w$ is the water phase compressibility, $c_m$ is the compressibility of the porous media, and $\phi_0$ is the porosity of the medium at $P_w = P_{w0}$.

## 3 DISCRETIZATION

A Galerkin finite element method is used to discretize the eqns, (1). An influence coefficient technique is employed to handle the non-linearities in the flow terms.[21] The time discretization is carried out with a backward Euler method, and mass lumping is used for the mass accumulation term. Further details about this method can be found in[10,11,16,27]

If $N_i$ are the usual Lagrange polynomial $C^0$ basis functions where

$$\begin{aligned} N_i &= 1 \text{ at node } i \\ &= 0 \text{ at all other nodes} \\ \sum_j N_j &= 1 \text{ everywhere in the solution domain} \end{aligned} \tag{7}$$

and we define $\psi_l = P_l - \rho_l g D$, then $P_l$, $\psi_l$, and $S_l$ are approximated by

$$\begin{aligned} P_l &= \sum_j P_{lj} N_j \\ \psi_l &= \sum_j \psi_{lj} N_j \\ &= \sum_j (P_{lj} - \rho_{lj} g D_j) N_j \\ S_l &= \sum_j S_{lj} N_j \end{aligned} \tag{8}$$

If $N$ denotes the time level, then the discrete equations for phase $l = w, a$ are

$$\begin{aligned} &\{[\phi S_l \rho_l]_i^{N+1} - [\phi S_l \rho_l]_i^N\} \frac{V_i}{\Delta t} \\ &= \sum_{j \in \eta_i} (\rho_l \lambda_l)_{(ij+1/2)}^{N+1} \gamma_{ij} (\psi_{lj}^{N+1} - \psi_{li}^{N+1}) + (q_l)_i^{N+1} V_i \\ &\quad + \int_s N_i (\rho_l \mathbf{V}_l)^{N+1} \cdot \hat{n} \, \mathrm{d}s \end{aligned} \tag{9}$$

where

$$\begin{aligned} V_i &= \int_v N_i \, \mathrm{d}v \\ \psi_{li}^{N+1} &= P_{li}^{N+1} - \rho_{l,ij+1/2}^{N+1} g D_i \\ \rho_{l,ij+1/2} &= (\rho_{l,i} + \rho_{l,j})/2 \end{aligned} \tag{10}$$

and the $\gamma_{ij}$ are given by

$$\gamma_{ij} = -\int_v \nabla N_i \cdot \mathbf{K} \cdot \nabla N_j \, \mathrm{d}v \tag{11}$$

Here $\eta_i$ is the set of neighbour nodes of node $i$ such that $\gamma_{ij}$ are non-zero.

In equation (9), the term

$$\int_s N_i (\rho_l \mathbf{V}_l)^{N+1} \cdot \hat{n} \, \mathrm{d}s \tag{12}$$

represents the flux into the domain due to specified flux (or pressure) boundary conditions ($s$ in eqn (9) is the surface of the computational domain). A specified pressure can always be enforced by injecting or producing mass into a node.[11,13,16,33]

Since this term simply represents mass inflow or outflow, we can lump this boundary flux in with the flux due to wells to get a composite source/sink term[11,13,16,33]

$$Q_{li}^{N+1} = (q_{li})^{N+1} V_i + \int_s N_i (\rho_l \mathbf{V}_l)^{N+1} \cdot \hat{n} \, \mathrm{d}s \tag{13}$$

Therefore, the final discrete equations are

$$\begin{aligned} &\{[\phi S_l \rho_l]_i^{N+1} - [\phi S_l \rho_l]_i^N\} \frac{V_i}{\Delta t} \\ &= \sum_{j \in \eta_i} (\rho_l \lambda_l)_{(ij+1/2)}^{N+1} \gamma_{ij} (\psi_{lj}^{N+1} - \psi_{li}^{N+1}) + (Q_l)_i^{N+1} \end{aligned} \tag{14}$$

Note that in eqn (10) there is a possible problem for the definition of $\rho_{l,ij+1/2}$, which appears in the gravity term, if a phase is not present in either node $i$ or node $j$ (this should not be confused with the term $\rho_l$ which multiplies the mobility term in eqn (14)). If phase $l$ is present in only one node, say node $i$, then in this case $\rho_{l,ij+1/2} = \rho_{l,i}$. If phase $l$ is not present in either node, then $\rho_{l,ij+1/2}$ is irrelevant since these terms are multiplied by a zero relative permeability.

There are various possibilities for the term $(\rho_l \lambda_l)_{(ij+1/2)}$ in eqn (14). Two weightings that will be used in this work are central (*cent*) and upstream (*ups*)

$$\begin{aligned} (\rho_l \lambda_l)_{ups(i,j)} &= (\rho_l \lambda_l)_i^{N+1} \text{ if } \gamma_{ij}(\psi_{lj}^{N+1} - \psi_{li}^{N+1}) < 0 \\ &= (\rho_l \lambda_l)_j^{N+1} \text{ if } \gamma_{ij}(\psi_{lj}^{N+1} - \psi_{li}^{N+1}) > 0 \\ (\rho_l \lambda_l)_{cent(i,j)} &= \left((\rho_l \lambda_l)_i^{N+1} + (\rho_l \lambda_l)_j^{N+1}\right)/2 \end{aligned} \tag{15}$$

Other possibilities include using an appropriate average of the values of $\lambda_l$ at the centroids of any elements which contribute to $\gamma_{ij}$.[21] Equation (15) amounts to using a one point quadrature method to evaluate the nonlinear term in the integral. For true two phase (non-constant air phase pressure) problems, upstream weighting can be shown to converge to the physically correct solution.[32] As demonstrated in Ref. 3, central weighting may cause convergence to incorrect solutions in multi-phase flow situations. Consequently, only upstream weighting will be used for active air phase computations. If the constant air phase pressure approximation is invoked, both central and upstream weighting will be used in this work.

Note that the discrete eqns (14) has the same form regardless of the dimensionality of the system or the type of basis function used. In fact, eqns (14) are also valid if a finite volume discretization is used.[8,9] In this case, the $V_i$ are the actual geometric volumes associated with the node, and $\gamma_{ij}$ is the interfacial area divided by the distance between nodes $i$ and $j$.

Of course, for a finite volume method, $\gamma_{ij} \geq 0$. This need not be the case for a finite element method.[11,16,27] If $\gamma_{ij} < 0$, then this can result in locally nonphysical discrete flow, which may cause poor convergence of the nonlinear iteration.[11,27] Requiring that $\gamma_{ij} \geq 0$ for a finite element method puts a constraint on the type of basis function and the node placement.[11,27]

Since $\gamma_{ij} = \gamma_{ji}$ it follows immediately from eqn (14) that this discretization is mass conservative.

## 4 MONOTONICITY CONSIDERATIONS

The importance of a monotone discretization has been pointed out by.[5,11,12] In the following, the definition of monotonicity is briefly reviewed and the implications of this requirement are considered. Only the discrete problem is considered for the constant air pressure approximation. In this case, the monotonicity analysis

can be carried out for the full nonlinear equations, and for any dimension.

If the air pressure is assumed to be constant, this eliminates the air conservation equation from the system of two eqns, (1), leaving only the water conservation equation. For definiteness, assume that the independent variables in the discrete algebraic system (14) are the water phase pressures $P_{wi}$. The nodal water saturation $S_{wi}$ is obtained by inverting eqn (4)

$$\begin{aligned} P_a &= \text{constant} \\ S_{wi} &= \min(1{\cdot}0, P_{caw}^{-1}(P_a - P_{wi})) \end{aligned} \tag{16}$$

Consequently, the discrete algebraic eqns (14) with the constraint equation (16) can be considered to be a set of discrete implicit algebraic equations specified at each node $i$, which can be written in the form

$$f_i(P_{wi}^{N+1}, P_{wi}^{N}, P_{wj}^{N+1}) = 0 \qquad j \in \eta_i \qquad \forall i \tag{17}$$

For the purposes of monotonicity analysis, the variables $P_{wi}^N$, $P_{wj}^{N+1}$ are regarded as independent.[12] We then require that

$$\begin{aligned} &\frac{\partial P_{wi}^{N+1}}{\partial P_{wi}^{N}} \geq 0 \\ &\frac{\partial P_{wi}^{N+1}}{\partial P_{wj}^{N+1}} \geq 0 \qquad \forall j \in \eta_i \end{aligned} \tag{18}$$

for every node $i$.

An intuitive explanation of this requirement is that a positive perturbation of the pressures at $P_{wi}^N$ or $P_{wj}^{N+1}$ should produce a positive change in $P_{wi}^{N+1}$. If positive perturbations of $P_{wi}^N$, $P_{wj}^{N+1}$ produce a negative perturbation of $P_{wi}^{N+1}$, then this is physically absurd.

Mathematically, the requirement (18) ensures that no new non-physical local maxima or minima can appear in the discrete solution $P_{wi}^{N+1}$ (i.e. nonphysical oscillations cannot occur). Note that new local maxima can occur at the nodes on the edge of the grid, or near heterogeneities (consider infiltration into a dry soil encountering an impermeable zone), but these local maxima are physically correct. A more precise statement of this condition is given in Forsyth and Kropinski[15] and Kropinski.[26]

Consequently, it is a straightforward, although algebraically tedious, matter to apply conditions (18) to the discrete system (14), bearing in mind the constraint (16).

Provided very mild restrictions are placed on the vertical dimension of the computational domain,[15,26] then the results of this analysis can be summarized as follows.[15,26] Let

$$\Delta x = \min_{i \neq j} (\|\mathbf{x}_i - \mathbf{x}_j\|) \tag{19}$$

where $\mathbf{x}_i$ is the location vector of node $i$. If the discretization of eqn (14) (with the passive air phase assumption) satisfies the following conditions

$$\begin{aligned} &\text{(a)} \quad \partial P_{caw}/\partial S_w < 0 \\ &\text{(b)} \quad \gamma_{ij} \geq 0 \text{ (see eqn (11))} \\ &\text{(c)} \quad \text{upstream weighting is used (eqn (15))} \end{aligned} \tag{20}$$

then the discretization (14) is unconditionally monotone regardless of timestep $\Delta t$ or mesh size $\Delta x$. This implies that non-physical oscillations in the solution cannot occur, no matter how large the mesh size or timestep.[15] Of course, accuracy considerations may put an upper limit on timestep or mesh sizes. However, in Ref. 15, an example is given where the non-monotone discretizations produce non-physical solutions even for very small mesh sizes. These non-physical oscillations are absent from monotone discretizations. If central weighting (or any other linear combination of mobilities which includes non-upstream nodes) is used, then the discretization is monotone only for sufficiently small $\Delta x$.[15] Note that (a) in (20) is satisfied for any physically reasonable capillary pressure function.

As mentioned in [7], the discretization will not be monotone, in general, if a consistent mass matrix is used. If higher order timestepping methods are employed, the discretization will also be non-monotone for large $\Delta t$. If the mobility term $\lambda_w$ is evaluated explicitly, as in Kirkland *et al.*[23] then the discretization is monotone only for sufficiently small $(\Delta t/\Delta x)$.

The choice of whether to use central or upstream weighting clearly depends on the grid size. For fine grids (see Refs 15 and 26 for a precise specification), central weighting will be monotone. However, for coarse grids, it may be preferable to have slightly diffused, but monotone solution, as opposed to a solution which is oscillatory.

Note that the definition of the upstream point (eqn (15)) is based purely on mathematical monotonicity conditions, not physical reasoning. In simple cases, this definition of upstream weighting agrees with physical intuition. For more complex grids (unstructured triangular or tetrahedral elements), various authors have proposed methods for upstream type weightings.[20] However it is not clear if these definitions of upstream weighting are monotone. In contrast, the definition (15) is monotone (provided conditions (a)–(b) in (20) are satisfied) for complex grids.

## 5 VARIABLE SUBSTITUTION

Numerical experience seems to suggest that use of a water content (or equivalently saturation) based form of Richards' equation has good convergence properties in terms of nonlinear iterations[19,23] compared to a pressure based method. Of course, the saturation based equation cannot be used in the saturated zone. This problem can be circumvented by defining a new variable which is

essentially the saturation in the unsaturated zone, and is the pressure in the saturated zone.[23] In Ref. 23, the equations are actually rewritten in terms of this new variable, which introduces some complications for heterogeneous systems. The technique used in Ref. 23 is also partially explicit, and so is not monotone unless $\Delta t/\Delta x$ is sufficiently small. Mass balance errors are also introduced at the transition between the saturated and unsaturated zones.

In this work, full Newton iteration will be used to solve the discrete eqn (14) everywhere. In the case of the constant air phase pressure approximation, we simply use a different primary variable in different regions (recall that the primary variables are those variables which are regarded as independent when constructing the Jacobian). The primary variable at any given node may be switched after every Newton iteration using the following method.

```
IF (S_wi ≥ tol_f) then
    Use P_wi as primary variable at node i
ELSEIF (S_wi < tol_b) then
    Use S_wi as primary variable for node i          (21)
ELSE
    Do not change primary variable for this node
ENDIF
```

Variable substitution is commonly used in multiphase, multicomponent flow to ensure that the Jacobian is nonsingular when phases appear and disappear due to mass transfer between phases.[8–10,13,16,17,33] In this work, we are simply using variable substitution to aid the convergence of the Newton iteration. Consequently, there is a great deal of freedom in the selection of the switching parameters $tol_b$ and $tol_f$. The only necessary requirement is that

$$tol_f < 1 \tag{22}$$

Note that in general $tol_f \neq tol_b$. This will be discussed further in subsequent sections.

We emphasize that the same discrete equations are being solved everywhere. Only the primary variable for the Newton iteration is being switched. This approach is designed to produce rapid convergence in both the unsaturated and saturated zones for all initial and transient conditions.

## 6 JACOBIAN CONSTRUCTION

At first sight the variable substitution method described above might appear to be difficult to implement. However, variable substitution is very straightforward to implement if the Jacobian is constructed numerically.[17] Consider the discrete eqns (14) with constraints (16) for a constant air phase pressure model. In this case, there is only one primary variable per node. Let $X_i$ be the primary variable associated with node $i$ ($X_i$ can be either $P_{wi}$ or $S_{wi}$ as determined by (21)). Let

$$\begin{aligned} A(X_i) &= \phi S_{wi}\rho_{wi}\frac{V_i}{\Delta t} \\ \text{flow}(X_j, X_i)_{ji} &= (\rho_w\lambda_w)^{N+1}_{(ij+1/2)}\gamma_{ij}(\psi^{N+1}_{wj} - \psi^{N+1}_{wi}) \\ Q(X_i) &= (Q_w)^{N+1}_i \end{aligned} \tag{23}$$

Then, determine $X_i$ such that the residual of the discrete equations is zero. In other words

$$\begin{aligned} r_i &= -(A_i^{N+1} - A_i^N) + \sum_j \text{flow}_{ji} + Q_i \\ &= 0 \qquad \forall i \end{aligned} \tag{24}$$

Utilizing the fact that the discretization (14) is conservative which means that

$$\text{flow}_{ij} = -\text{flow}_{ji} \tag{25}$$

and that $\text{flow}_{ij}$ is only a function of $X_i$, $X_j$, then the Jacobian $J_{ij}$ can then be constructed using the following algorithm. The notation $X_i$ refers to the current value (at this iteration) of the solution for $X_i^{N+1}$.

```
FOR i = 1,...,
  sum := 0
  FOR j ∈ η_i
      J_ji := flow (X_j, X_i)_ji
      sum := sum + flow (X_j, X_i)_ji
  ENDFOR
  sum := sum − (A(X_i) − A(X_i^N)) + Q(X_i)
  J_ii := sum
  r_i := sum                                          (26)
  sum := 0
  FOR j ∈ η_i
      J_ji := (J_ji − flow (X_j, X_i + ε))/ε
      sum := sum + flow (X_j, X_i + ε)_ji
  ENDFOR
  sum := sum − (A(X_i + ε) − A(X_i^N)) + Q(X_i + ε)
  J_ii := (sum − J_ii)/ε
ENDFOR
```

where $\epsilon$ is a suitably determined numerical shift factor. Of course if $\epsilon$ is chosen too small, then roundoff errors will result, while if $\epsilon$ is too large, then this will be a poor approximation to the Jacobian. Assuming that the primary variables are $O(1)$, then a useful rule of thumb is to select the shift factor $\epsilon$ to be the square root of the unit roundoff. For example, if double precision arithmetic is used, with the unit roundoff being about $10^{-12}$, then $\epsilon = 10^{-6}$ would be a reasonable choice. We have experimented with various values of $\epsilon$ over several years, and we have always observed quadratic convergence for the Newton iteration (as convergence is approached) for the above choice for $\epsilon$.

Some of the correlations typically used[31] for relative permeabilities and capillary pressures have infinite derivatives as $S_w$ tends to the residual value or to unity. In this case, the correlation is replaced by a linear

interpolant for saturation values near these troublesome points. The derivatives now become large but finite. For example, whenever $S_w > 1 - \epsilon_1$, a linear interpolant is used. The value of $\epsilon_1$ is selected to be an order of magnitude smaller than the saturation convergence tolerance. Experiments with smaller values of $\epsilon_1$ did not change the solution to within the convergence tolerance.

Note that if upstream weighting is used, then it is important to base the upstream decision (15) on the unincremented values $(X_i)$, *not* the incremented values $(X_i + \epsilon)$ of the primary variables.

The above algorithm constructs the Jacobian by columns. Consequently, the residual and the entire Jacobian can be constructed in a cost equivalent to two residual evaluations. Note that this is true regardless of the dimensionality or number of nonzeros in the Jacobian. For clarity, the above algorithm is written as if $J_{ij}$ was stored in full form. Of course, in practice, $J_{ij}$ is stored in packed form.

In the case of multiphase flow with $n_p$ phases, the residual and the Jacobian can be computed numerically at a cost of $n_p + 1$ residual evaluations.

## 7 MATRIX SOLUTION AND TIMESTEPPING

The non-symmetric Jacobian matrix is solved using an iterative method based on a reduced system, level (1) incomplete factorization,[4,6,35] with CGSTAB acceleration.[7] A standard adaptive timestepping method is used to control the timestep size.[34]

## 8 TEST PROBLEMS

All capillary pressures and relative permeabilities are assumed to be of the van Genuchten[31] form

$$\begin{aligned} P_{caw} &= \frac{\rho_w g}{\alpha}\left((\bar{S}_w)^{-1/\gamma} - 1\right)^{1/\beta} \\ \bar{S}_w &= \frac{S_w - S_{wr}}{1 - S_{wr}} \\ \gamma &= 1 - \frac{1}{\beta} \end{aligned} \tag{27}$$

The relative permeabilities are given by

$$\begin{aligned} k_{rw} &= (\bar{S}_w)^{1/2}\{1 - [1 - (\bar{S}_w)^{1/\gamma}]^{\gamma}\}^2 \\ k_{ra} &= (\bar{S}_a)^{1/2}\{1 - (\bar{S}_w)^{1/\gamma}\}^{2\gamma} \\ \bar{S}_a &= 1 - \bar{S}_w \end{aligned} \tag{28}$$

In order to ensure that the air phase pressure remained approximately constant for the full two phase flow formulations, additional constant pressure air boundaries (seepage points) were imposed on the upper surfaces of the computational domains. The location of these constant pressure nodes is given for each test problem. In the following examples, water and porous media compressibilities are assumed zero, i.e. (see eqn (6)).

$$\begin{aligned} c_m &= 0 \\ c_w &= 0 \end{aligned} \tag{29}$$

**Table 1. Material properties for Problem 1 (Bandelier Tuff)**

| $K_x = K_y$ (m$^2$) | $\phi$ | $S_{wr}$ | $\alpha$ (1/cm) | $\beta$ |
|---|---|---|---|---|
| $2{\cdot}95 \times 10^{-13}$ | 0·33 | 0·0 | 0·0143 | 1·506 |

### 8.1 Problem 1

The first example is a one dimensional problem used to validate the HYDRUS code,[24] involving infiltration in a large caisson. This example is not particularly difficult, since the initial conditions are not very dry. However, this problem is included (and comparison with the HYDRUS code), to justify the use of full Newton iteration, as opposed to the Picard scheme used in HYDRUS. The experimental study was conducted at Los Alamos National Laboratory.[1,2] Table 1 gives the material properties used in this simulation. These properties are those of Bandelier Tuff. Figure 1 shows the computational domain for this one dimensional

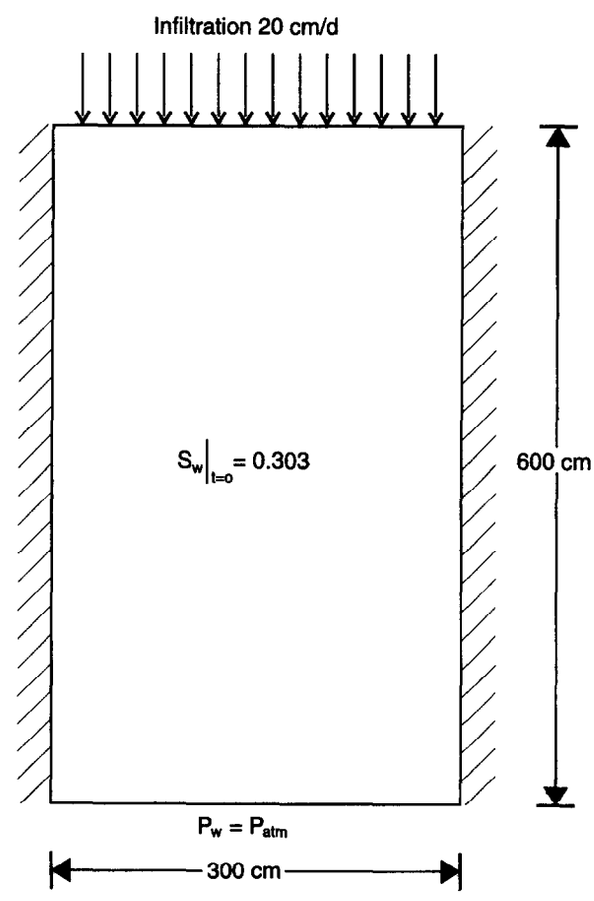


**Fig. 1.** Domain for Test Problem 1.

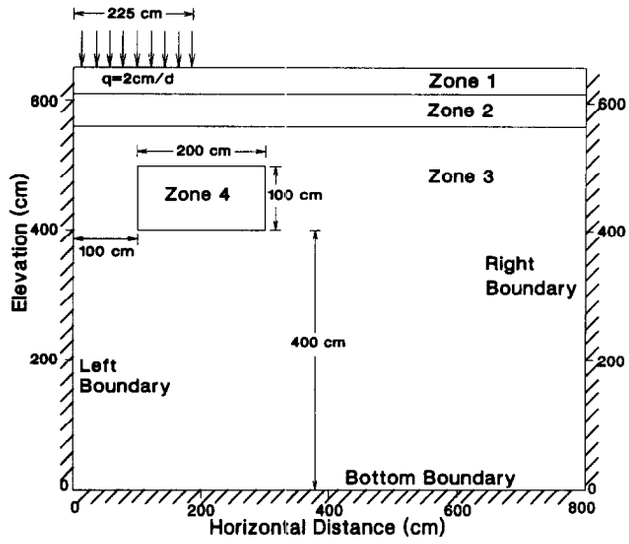


**Fig. 2.** Domain for Test Problem 2.

example, which is a caisson 6 m long and 3 m in diameter. A node spacing of 5 cm (120 nodes) was used in the $z$ direction. The water saturation was initially $S_w = 0{\cdot}303$ everywhere. The model was run for 7·16 days.

### 8.2 Problem 2

The second test example is the problem which was developed to compare the performance of numerical simulators for the very dry initial conditions.[36] The computational domain is shown in Fig. 2. All boundaries are no flow, except for the zone of infiltration as shown in Fig. 2 (2 cm/day). Table 2 shows the material properties for Problem 2. Note that Zones 3 and 4 differ only in the absolute permeabilities. For the full two phase formulations, a constant air pressure boundary condition was imposed at the top right hand corner.

A $90 \times 21$ finite volume grid was used for this problem (1890 nodes). Problem 2 uses an initial condition of $P_w = 28{\cdot}0$ kPa (or in terms of head, $h_i = -734$ cm-water). Water infiltration occurs for 30 days.

### 8.3 Problem 3

This problem is the same as Problem 2, except that the initial absolute water pressure is $P_w = -880{\cdot}665$ kPa (in terms of head $h_i = -10\,000$ cm-water). Problem 3 can be

**Table 2. Material properties for Problem 2**

| Zone | $K_x = K_y$ (m$^2$) | $\phi$ | $S_{wr}$ | $\alpha$ (1/cm) | $\beta$ |
|---|---|---|---|---|---|
| 1 | $9{\cdot}33 \times 10^{-12}$ | 0·3680 | 0·2771 | 0·0334 | 1·982 |
| 2 | $5{\cdot}55 \times 10^{-12}$ | 0·3510 | 0·2806 | 0·0363 | 1·632 |
| 3 | $4{\cdot}898 \times 10^{-12}$ | 0·3250 | 0·2643 | 0·0345 | 1·573 |
| 4 | $4{\cdot}898 \times 10^{-11}$ | 0·3250 | 0·2643 | 0·0345 | 1·573 |

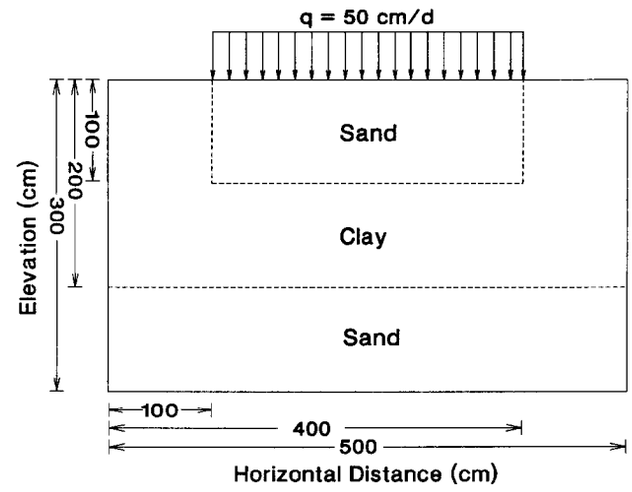


**Fig. 3.** Domain for Test Problem 4.

expected to be more difficult than Problem 2 since the initial water saturation will be smaller, which will cause sharp moving fronts.

### 8.4 Problem 4

This example is Test Problem 2 in Ref. 23. The computational domain is shown in Fig. 3. A $100 \times 60$ (6000 nodes) finite volume grid was used for this problem, no advantage was taken of the obvious symmetry. This problem models one day of water injection. The material properties for this problem are given in Table 3. All boundaries are no flow except where the infiltration is shown in Fig. 3. The initial pressure was $P_w = -4800$ kPa. For the full two phase formulation, constant air pressure boundary conditions were imposed on the top left and top right corners of the domain.

Note that this problem was designed so that water initially infiltrates into a dry soil, but then encounters a clay barrier which causes formation of a perched water table. Many nodes become saturated with water, so that this problem is a good test of the formulation's ability to handle both very dry conditions, and then to make the transition to a saturated state.

### 8.5 Problem 5

This problem is a three dimensional version of Problem 3. A $46 \times 46 \times 21$ (44 436 nodes) tetrahedral finite element discretization was employed. A cross section of the problem domain is shown in Fig. 4. Note that an additional impermeable zone has been added below the water injection.

**Table 3. Material Properties for Problem 4**

| Material | $K_x = K_y$ (m$^2$) | $\phi$ | $S_{wr}$ | $\alpha$ (1/cm) | $\beta$ |
|---|---|---|---|---|---|
| Clay | $1{\cdot}546 \times 10^{-13}$ | 0·4686 | 0·2262 | 0·0104 | 1·3954 |
| Sand | $6{\cdot}385 \times 10^{-12}$ | 0·3658 | 0·07818 | 0·0280 | 2·239 |

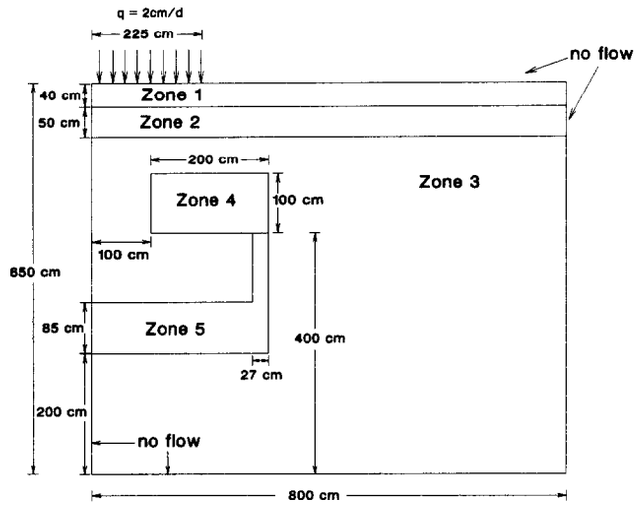


**Fig. 4.** Cross section for Test Problem 5.

All boundaries are no flow except where the infiltration is indicated (2 cm/day). The infiltration occurs over the surface area

$$z = 6{\cdot}5\,\mathrm{m} \qquad 0{\cdot}0 \le x \le 2{\cdot}25\,\mathrm{m} \qquad 0{\cdot}0 \le y \le 2{\cdot}25\,\mathrm{m} \tag{30}$$

The material properties are the same as in Table 2, except for Zone 5 (see Table 4).

The problem domain is

$$\begin{aligned} &0 \le x \le 8{\cdot}0\,\mathrm{m} \\ &0 \le y \le 8{\cdot}0\,\mathrm{m} \\ &0 \le z \le 6{\cdot}5\,\mathrm{m} \end{aligned} \tag{31}$$

The various zones are

$$\begin{aligned} &\text{Zone 1} \quad 0{\cdot}0\,\mathrm{m} \le x \le 8{\cdot}0\,\mathrm{m};\ 0{\cdot}0\,\mathrm{m} \le y \le 8{\cdot}0\,\mathrm{m}; \\ &\qquad\qquad 6{\cdot}1\,\mathrm{m} \le z \le 6{\cdot}5\,\mathrm{m} \\ &\text{Zone 2} \quad 0{\cdot}0\,\mathrm{m} \le x \le 8{\cdot}0\,\mathrm{m};\ 0{\cdot}0\,\mathrm{m} \le y \le 8{\cdot}0\,\mathrm{m}; \\ &\qquad\qquad 5{\cdot}6\,\mathrm{m} \le z \le 6{\cdot}1\,\mathrm{m} \\ &\text{Zone 4} \quad 1{\cdot}0\,\mathrm{m} \le x \le 3{\cdot}0\,\mathrm{m};\ 1{\cdot}0\,\mathrm{m} \le y \le 3{\cdot}0\,\mathrm{m}; \\ &\qquad\qquad 4{\cdot}0\,\mathrm{m} \le z \le 5{\cdot}0\,\mathrm{m} \\ &\text{Zone 5} \quad 0{\cdot}0\,\mathrm{m} \le x \le 3{\cdot}0\,\mathrm{m};\ 0{\cdot}0\,\mathrm{m} \le y \le 3{\cdot}0\,\mathrm{m}; \\ &\qquad\qquad 2{\cdot}0\,\mathrm{m} \le z \le 2{\cdot}85\,\mathrm{m};\ 2{\cdot}73\,\mathrm{m} \le x \le 3{\cdot}0\,\mathrm{m}; \\ &\qquad\qquad 0{\cdot}0\,\mathrm{m} \le y \le 3{\cdot}0\,\mathrm{m};\ 2{\cdot}85\,\mathrm{m} \le z \le 4{\cdot}0\,\mathrm{m}; \\ &\qquad\qquad 2{\cdot}73\,\mathrm{m} \le y \le 3{\cdot}0\,\mathrm{m};\ 0{\cdot}0\,\mathrm{m} \le x \le 3{\cdot}0\,\mathrm{m}; \\ &\qquad\qquad 2{\cdot}85\,\mathrm{m} \le z \le 4{\cdot}0\,\mathrm{m} \\ &\text{Zone 3} \quad \text{everywhere else} \end{aligned} \tag{32}$$

The initial pressure was $-880{\cdot}67$ kPa everywhere.

**Table 4. Material Properties for Problem 5**

| Zone | $K_x = K_y$ (m$^2$) | $\phi$ | $S_{wr}$ | $\alpha$ (1/cm) | $\beta$ |
|---|---|---|---|---|---|
| 5 | $1{\cdot}0 \times 10^{-14}$ | 0·3250 | 0·2643 | 0·0345 | 1·573 |

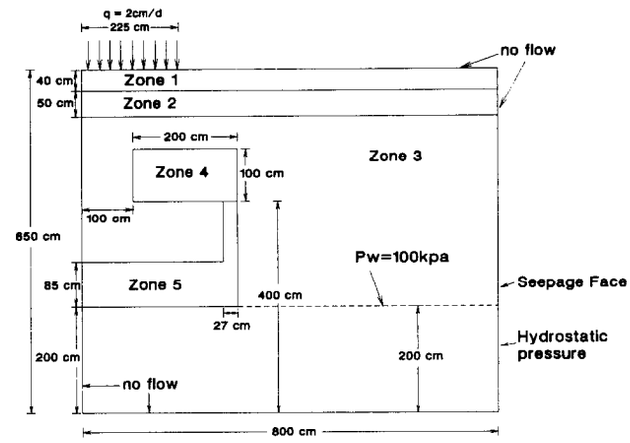


**Fig. 5.** Cross section for Test Problem 6.

### 8.6 Problem 6

This problem is essentially the same as Problem 5, except that initially the water table is at $z = 200$ cm (see Fig. 5), and both hydrostatic and seepage face conditions are imposed at one end of the domain (see Fig. 5). In the unsaturated zone, the initial absolute water pressure is $P_w = 28{\cdot}01$ kPa. More precisely, the initial conditions are

$$\begin{aligned} P_w &= 28{\cdot}01\,\mathrm{kPa} \qquad 2{\cdot}0\,\mathrm{m} \le z \le 6{\cdot}5\,\mathrm{m} \\ P_w &= 100\,\mathrm{kPa} \qquad 0{\cdot}0\,\mathrm{m} \le z \le 2{\cdot}0\,\mathrm{m} \end{aligned} \tag{33}$$

All boundaries are the same as for Problem 5, except that the plane $x = 6{\cdot}5$ m has

$$\begin{aligned} P_w &= 100\,\mathrm{kPa} \qquad z = 2{\cdot}0\,\mathrm{m} \\ &= \text{hydrostatic} \qquad 0{\cdot}0\,\mathrm{m} \le z \le 2{\cdot}0\,\mathrm{m} \\ &\text{Seepage face} \qquad 2{\cdot}0\,\mathrm{m} \le z \le 6{\cdot}5\,\mathrm{m} \end{aligned} \tag{34}$$

## 9 RESULTS

For the variable substitution (constant air phase pressure) and the two phase (non-constant air phase pressure) formulations, very aggressive timestep selector targets[34] were used: 0·40 for the saturation, and 4000 kPa for the pressure. Various tests were carried out with smaller timesteps. Saturation contour plots of the small timestep results at the end of the simulation time compared to plots with the aggressive timestep strategy were virtually identical. Consequently, results will be reported only for the aggressive timestep strategy.

For the constant air phase formulation, using only the pressure as a primary variable, an aggressive timestepping strategy performed very poorly due to convergence failures of the Newton iteration. For each test problem, it was necessary to tune the timestep selector parameters by trial and error. Results will be reported for the best choice of timestep parameters.

If $tol_f = tolf_b$ in eqn (21), this sometimes caused the

Newton iteration to oscillate between the two states with different primary variables. This problem was eliminated if $tol_f \neq tol_b$. The parameters that were used in the work were

$$tol_f = 0{\cdot}99 \qquad tol_b = 0{\cdot}89 \tag{35}$$

Since a mass conservative formulation is used in all cases, the material balance error is simply a function of the convergence tolerance. Material balance errors in all cases were less than $5 \times 10^{-5}$. In the following, variable substitution refers to the method of eqn (21) using the constant air phase approximation. If the same set of equations are solved using $P_w$ as a primary variable, this method will be referred to as $P_w$ primary variable, while two phase indicates that the true two phase equations are solved (non-constant air phase pressure). For the two phase runs, $P_w$ and $S_w$ were selected as the primary variables.

Since a variety of different machines were used at different sites, we give the normalized CPU time if available. The two phase (non-constant air phase pressure) runs were carried out using the MAGNAS code[22] on a different machine from any other runs, so CPU times are not meaningful.

### 9.1 Results for Problem 1

Figure 6(a) shows the water saturation contours at various times. The results for both central and upstream weighting (using the constant air phase approximation) are compared with the HYDRUS simulation. This problem was solved using both central and upstream weighting, using variable substitution and $P_w$ primary variable. As can be seen in Fig. 6(a), all methods are in close agreement with the HYDRUS mass conservative, centrally weighted, results.[24] The difference between central and upstream weighting is very small. In fact, the difference between central and upstream weighting is much less than the difference between using a mass conservative and a non-mass conservative formulation (both with central weighting) as described in Kool and van Genuchten.[24] However, the more interesting results are in Table 5.

The heading nonlinear iterations in Table 5 refers to the total number of Picard iterations for HYDRUS, and the total number of Newton iterations for the present model. Even accounting for the fact that construction of the Jacobian is more expensive than the construction of the Picard iteration matrix (at worst, using method (21), a factor of two), we can see that the Hydrus run is easily 10 times more expensive than the present method (using variable substitution). The initial conditions for this problem are not particularly dry, so the difference between using variable substitution and $P_w$ primary variable is not that pronounced. Nevertheless, in all cases, the variable substitution requires fewer Newton iterations than the corresponding $P_w$ primary variable runs. The next examples will show a much greater efficiency for variable substitution. The second part of this test problem involves simulation of the caisson drainage (by gravity), following complete saturation. All the conditions and parameters are the same as before, except that the top surface is treated as a zero flux boundary. Drainage was simulated for a period of 100 days, and the predicted water content at 1, 4, 20 and 100

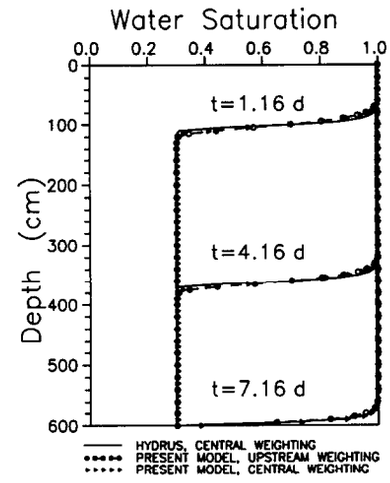


**Fig. 6(a).** Saturation contours, Problem 1.

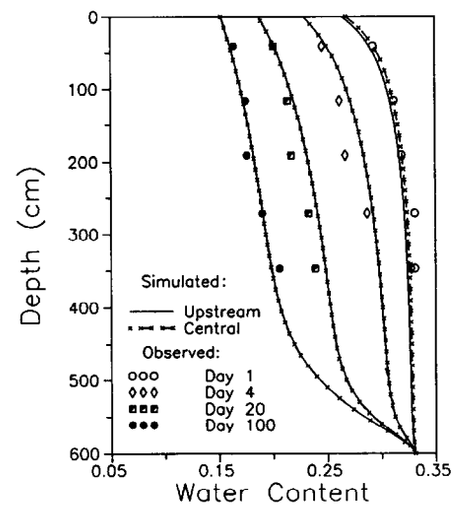


**Fig. 6(b).** Comparison of predicted and observed water content during drainage.

**Table 5. Results for Problem 1**

| Method | Weighting | Nonlinear iterations | Normalized CPU time |
|---|---|---|---|
| Variable substitution[a] | upstream | 178 | 1·0 |
| Variable substitution[a] | central | 273 | 1·46 |
| $P_w$ primary variable[b] | upstream | 251 | 1·28 |
| $P_w$ primary variable[b] | central | 362 | 1·79 |
| HYDRUS | central | 4886 | [c] |

[a] Constant air phase pressure using variable substitution.
[b] Constant air phase pressure, $P_w$ primary variable.
[c] Computation carried out on different architecture.

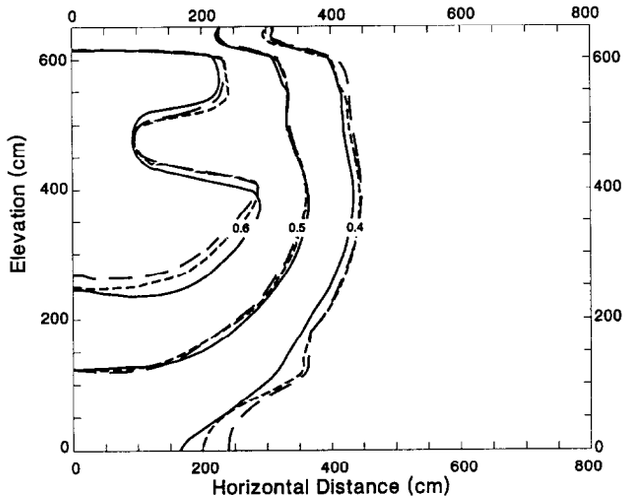


**Fig. 7.** Saturation contours, Problem 2. – – – One phase, upstream weighting; - - - - one phase, central weighting; —— two phase, upstream weighting.

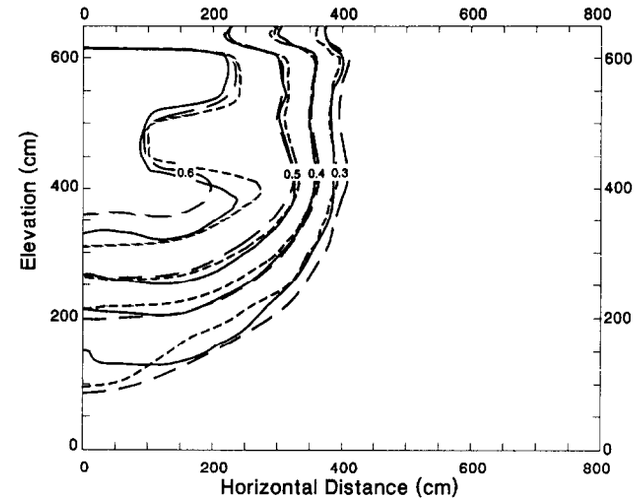


**Fig. 8.** Saturation contours, Problem 3. – – – One phase, upstream weighting; - - - - one phase, central weighting; —— two phase, upstream weighting.

days is given in Fig. 6(b). The experimentally observed[24] values of water content versus time are also shown. The numerical predictions are in good agreement with the experiment.

### 9.2 Results for Problem 2

Figure 7 shows the saturation contours for Problem 2 (at 30 days) obtained using a full two phase model, and a constant air phase approximation (labeled one phase in Fig. 7) with both central and upstream weighting. All methods are in fairly close agreement. The most noticeable difference occurs for the $S_w = 0{\cdot}4$ contour along the bottom edge. It is interesting to observe that the $S_w = 0{\cdot}4$ contour for the upstream weighted (constant air phase pressure) is slightly ahead of the same contour for the centrally weighted (constant air phase pressure) along the bottom edge. This might be expected due to the diffusive nature of upstream weighting. However, the centrally weighted (constant air phase pressure) $S_w = 0{\cdot}4$ contour is slightly ahead of the two phase (upstream weighted) $S_w = 0{\cdot}4$ contour. Note that nonlinear two phase shocks are self-sharpening, so that upstream weighting for two phase (non-constant air phase pressure) does not appear to be overly diffusive.[14] Table 6 gives the computational statistics for this problem. In this case, the $P_w$ primary variable method is between six and eight times slower than using variable substitution. This increase in computational cost is a direct result in the large increase in the number of Newton iterations required for the $P_w$ primary variable methods. Observe that the number of Newton iterations for the full two phase formulation is comparable with the number of Newton iterations for the variable substitution technique. Of course, the cost of each Newton iteration for the two phase method is greater than the cost of a Newton iteration with a constant air phase approximation.

### 9.3 Results for Problem 3

Figure 8 shows the saturation contours for Problem 3, using all three methods. Again, all three methods produce similar results. The $S_w = 0{\cdot}3$ contour for the upstream weighted (constant air phase pressure, labeled one phase in Fig. 8) is slightly diffused compared to the centrally weighted $S_w = 0{\cdot}3$ contour (constant air phase pressure). However, the upstream weighted two phase (non-constant air phase pressure) $S_w = 0{\cdot}3$ contour again appears to be slightly less diffused than the

**Table 6. Results for Problem 2**

| Method | Weighting | Nonlinear iterations | Inner iterations | Normalized CPU time |
|---|---|---|---|---|
| Variable substitution[a] | upstream | 31 | 137 | 1·0 |
| Variable substitution[a] | central | 29 | 141 | 1·02 |
| $P_w$ primary variable[b] | upstream | 207 | 725 | 6·2 |
| $P_w$ primary variable[b] | central | 267 | 827 | 8·03 |
| Two phase[c] | upstream | 31 | 113 | [d] |

[a] Constant air phase pressure using variable substitution.
[b] Constant air phase pressure, $P_w$ primary variable.
[c] Two phase active air phase.
[d] Computation carried out on different architecture.

**Table 7. Results for Problem 3**

| Method | Weighting | Nonlinear iterations | Inner iterations | Normalized CPU time |
|---|---|---|---|---|
| Variable substitution[a] | upstream | 50 | 244 | 1·0 |
| Variable substitution[a] | central | 48 | 259 | 1·04 |
| $P_w$ primary variable[b] | upstream | 450 | 1428 | 7·08 |
| $P_w$ primary variable[b] | central | 512 | 1802 | 8·7 |
| Two phase[c] | upstream | 67 | 175 | [d] |

[a,b,c,d] See footnote to Table 6.

centrally weighted constant air phase pressure computation. The statistics for these runs are given in Table 7. In this case, the variable substitution methods are between seven and nine times faster than using the $P_w$ primary variable.

Note that for both Problems 2 and 3, the variable substitution method always uses $S_w$ as the primary variable, since the water saturation is always much less than one. Problems 4 and 6 both have large fully saturated zones, and consequently are good nontrivial examples of variable substitution.

### 9.4 Results for Problem 4

Figure 9 gives the saturation contours for all three methods. Although the contours are quite similar at small saturations, the $S_w = 0{\cdot}9$ and $S_w = 1{\cdot}0$ contours show significant differences. The upstream and centrally weighted computations (constant air phase pressure, labeled one phase in Fig. 9) are qualitatively similar, but with the upstream contours shifted downward slightly compared to the central weighted results. However, the two phase contours are qualitatively different from the constant air phase pressure computations. Since the van Genuchten air relative permeability curve[31] is quite flat near $S_a = 0$, we can expect that the true two phase solution will have a rarefaction behind the shock, while the constant air phase pressure solution will produce only a large shock.[14] Table 8 summarizes the computational statistics for this problem. Note that this problem has a very large infiltration rate.

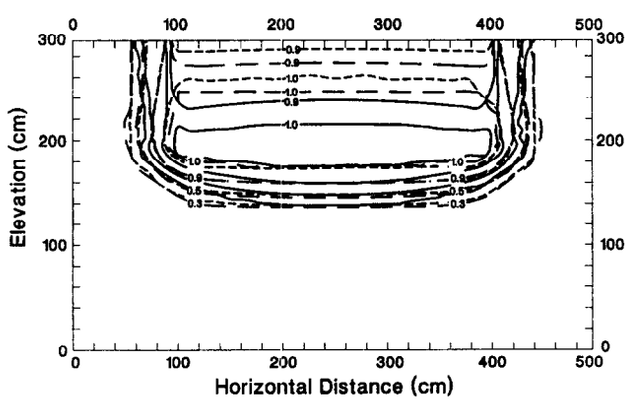


**Fig. 9.** Saturation contours, Problem 4. – – – One phase, upstream weighting; - - - - one phase, central weighting; —— two phase, upstream weighting.

In this case, the variable substitution method is about six times less costly than using $P_w$ as a primary variable.

### 9.5 Results for Problems 5 and 6

Figures 10 and 11 show saturation isosurfaces for the three dimensional test Problems 5 and 6. Note that Fig. 11 shows a multiply connected isosurface since water flows up from the saturated zone and down from the infiltration site. Table 9 summarizes the efficiency considerations for these problems. Since Problem 5 has more nodes with dry conditions than Problem 6, the variable substitution method is about nine times more efficient than the $P_w$ primary variable technique, compared with a factor of only about five to six for Problem 6. The two phase method was not run for these problems due to the large CPU cost required.

## 10 DISCUSSION

It is worthwhile at this point to summarize the results. For either central or upstream weighting, use of the standard $P_w$ primary variable method requires an order of magnitude more Newton iterations compared to the variable substitution method, if the initial conditions are dry. This translates into a decrease in CPU time of between five and nine times. For problems which are comparatively easy, i.e. the initial state is not very dry, the variable substitution method is still superior to $P_w$ primary variable, but only by about 30%. Of course, if the computational domain is entirely saturated, there is no difference between variable substitution and $P_w$ primary variable.

If the two phase (non-constant air phase) equations are solved, then the number of Newton iterations required is comparable to the number required for the variable substitution method. This indicates that the two phase formulation of these problems results in a set of discrete equations which is easy to solve. In the two phase formulation, one phase (either water or air) must be mobile. Hence, the derivative of the mass accumulation term with respect to $S_w$ is large, and contributes to the diagonal of the Jacobian. On the other hand, if the constant air phase formulation is used and the water is nearly immobile, then the derivative of the mass accumulation term with respect to $P_w$ is very small,

**Table 8. Results for Problem 4**

| Method | Weighting | Nonlinear iterations | Inner iterations | Normalized CPU time |
|---|---|---|---|---|
| Variable substitution[a] | upstream | 120 | 544 | 1·0 |
| Variable substitution[a] | central | 129 | 582 | 1·08 |
| $P_w$ primary variable[b] | upstream | 772 | 1843 | 6·3 |
| $P_w$ primary variable[b] | central | 797 | 1964 | 6·5 |
| Two phase[c] | upstream | 180 | 572 | [d] |

[a,b,c,d] See footnote to Table 6.

and hence this term hardly contributes to the diagonal of the Jacobian at all. This would appear to cause great difficulties for the Newton iteration if the $P_w$ primary variable method is employed. Although the derivative of the mass accumulation term with respect to $P_w$ may also be small as $S_w \to 1$, in this case there must be mobile water upstream of this node. This will result in a nonzero derivative of the flow term with respect to the pressure, so that the diagonal of the Jacobian will not be small.

Although the method used in Ref. 23 is similar in philosophy to the variable substitution method used here, there are some important differences. The variable substitution method used in the present work is mass conservative, is strictly monotone (if upstream weighting is used) for any timestep or mesh size, requires no special treatment of discontinuities in physical properties, and can be easily implemented in either finite element or finite volume codes.

## 11 CONCLUSIONS

The usual approach for solving saturated–unsaturated flow problems with the constant air phase pressure approximation uses the pressure (or head) as a primary variable. For infiltration into very dry soils, this method requires very small timesteps due to Newton iteration convergence problems. These timesteps are smaller than is required for reasonable time truncation errors. However, if variable substitution is used for the primary variable set, then the number of Newton iterations is reduced by an order of magnitude. On a series of test problems, we have demonstrated that the variable substitution method is between five and nine times faster (in terms of CPU time) than the usual pressure primary variable method, for dry initial conditions.

We emphasize here that the same set of discrete equations are being solved, only the method being used to solve the non-linear algebraic equations is different. If a numerical method is used for Jacobian construction, it is a very simple matter to change existing codes so that variable substitution is used instead of the pressure primary variable alone.

The order of magnitude improvement of variable substitution methods over pressure primary variable methods has been shown for both two and three

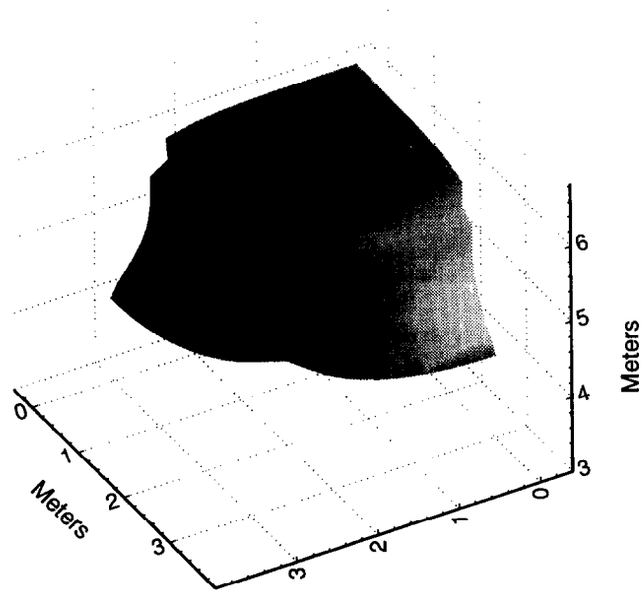


**Fig. 10.** Saturation isosurface, Problem 5, 30 days. $S_w = 0{\cdot}6$ isosurface.

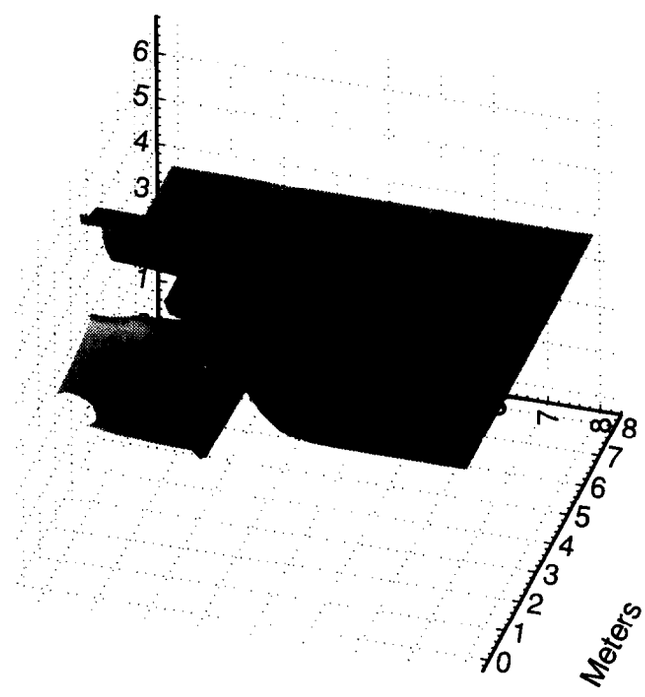


**Fig. 11.** Saturation isosurface, Problem 6, 30 days. $S_w = 0{\cdot}5$ isosurface.

**Table 9. Results for Problems 5 and 6**

| Method | Weighting | Nonlinear iterations | Inner iterations | Normalized CPU time |
|---|---|---|---|---|
| *Test Problem 5* | | | | |
| Variable substitution[a] | upstream | 58 | 236 | 1·0 |
| Variable substitution[a] | central | 61 | 266 | 1·1 |
| $P_w$ primary variable[b] | upstream | 599 | 1971 | 9·4 |
| $P_w$ primary variable[b] | central | 706 | 2278 | 9·65 |
| *Test Problem 6* | | | | |
| Variable substitution[a] | upstream | 39 | 353 | 1·0 |
| Variable substitution[a] | central | 41 | 333 | 0·90 |
| $P_w$ primary variable[b] | upstream | 308 | 1704 | 5·6 |
| $P_w$ primary variable[b] | central | 328 | 1787 | 5·9 |

[a,b] See footnote to Table 5.

dimensional problems, finite element and finite volume discretizations, and central and upstream weighting. Note that the discretizations used here are mass conservative everywhere, are strictly monotone if upstream weighting is used, and are monotone for central weighting if the mesh is sufficiently fine.

The two phase (non-constant air phase pressure) runs were also in good agreement with the computations which used the constant air phase pressure approximation, except for the situation where the infiltrating water saturation was near one. In this case, due to the trapping of the air phase, significant differences were observed between the active and passive air phase pressure results.

Finally, observe that the two phase (non-constant air phase pressure) equations were always easy to solve numerically, even for very dry, heterogeneous problems. It is interesting to note that a straightforward numerical approach which solves the physically more correct two phase flow equations generates algebraic equations which cause no difficulty for Newton iteration. This contrasts with the supposedly simplified constant air phase pressure equations, which can be very difficult to solve unless special care is taken.

## ACKNOWLEDGEMENTS

This work was supported by the Applied Mathematical Sciences subprogram of the Office of Energy Research, US Department of Energy, under contract DE-AC05-84OR21400 with Martin Marietta Energy Systems, Inc.; by HydroGeoLogic Inc., Herndon, VA; and by the director of Civilian Radioactive Waste Management, Office of External Relations, administered by the Nevada Operations Office in cooperation with the Swiss National Cooperative for the Disposal of Radioactive Waste (NAGRA), through US Department of Energy Contract No. DE-AC03-76SF00098. The authors would also like to thank J. B. Kool for use of data from HYDRUS simulations.

## REFERENCES

1. Abeele, W. V., Hydraulic Testing of Bandelier Tuff. Los Alamos National Laboratory Report LA-10037, 1984.
2. Abeele, W. V., Wheeler, M. L. & Burton, B. W., Geohydrology of Bandelier Tuff. Los Alamos National Laboratory Report LA-8962, 1981.
3. Aziz, K. & Settari, A., *Petroleum Reservoir Simulation.* Academic Press, NY, USA, 1979.
4. Behie, G. A. & Forsyth, P. A., Incomplete factorization methods for fully implicit simulation of enhanced oil recovery. *SIAM J. Sci. Stat. Comp.*, **5** (1984) 543–61.
5. Celia, M. A., Boultoulas, E. T. & Zarba, R. L., A general mass-conservative numerical solution method for the unsaturated flow equation. *Water Resour. Res.*, **26** (1990) 1483–96.
6. D'Azevedo, E.F., Forsyth, P. A. & Tang, W. P., Ordering methods for preconditioned conjugate gradient methods applied to unstructured grid problems. *SIAM J. Matrix Anal. Applic.*, **13** (1992) 944–61.
7. D'Azevedo, E. F., Forsyth, P. A. & Tang, W. P., Towards a cost effective ILU preconditioner with high level fill. *BIT*, **32** (1992) 442–63.
8. Falta, R. W., Pruess, K., Javandel, I. & Witherspoon, P., Numerical modelling of steam injection for the removal of nonaqueous phase liquids from the subsurface 1. Numerical formulation. *Water Resour. Res.*, **28** (1992) 433–49.
9. Falta, R., Javandel, I., Pruess, K. & Witherspoon, P., Density driven flow of gas in the unsaturated zone due to evaporation of volatile organic compounds. *Water Resour. Res.*, **25** (1989) 2159–69.
10. Forsyth, P. A., A positivity preserving method for simulation of steam injection for NAPL site remediation. *Adv. Water Res.*, **16** (1993) 351–70.
11. Forsyth, P. A., A control volume finite element approach to napl groundwater contamination. *SIAM J. Sci. Stat. Comp.*, **12** (1991) 1029–57.
12. Forsyth, P. A., Adaptive implicit criteria for two phase flow with gravity and capillary pressure. *SIAM J. Sci. Stat. Comp.*, **10** (1989) 227–52.
13. Forsyth, P. A., Simulation of nonaqueous phase groundwater contamination. *Adv. Water Res.*, **11** (1988) 74–83.
14. Forsyth, P. A., Comparison of single phase and two phase numerical model formulation for saturated–unsaturated groundwater flow. *Comp. Meth. Appl. Mech. Eng.*, **69** (1988) 243–59.
15. Forsyth, P. A. & Kropinski, M. C., Monotonicity Conditions for Saturated–Unsaturated Flow. University of Waterloo, Department of Computer Science Report CS-94-17, Canada.

16. Forsyth, P. A. & Shao, B. Y., Numerical simulation of gas venting for NAPL site remediation. *Adv. Water Res.*, **14** (1991) 354–67.
17. Forsyth, P. A. & Simpson, R.B., A two phase, two component model for natural convection in a porous medium. *Int. J. Num. Meth. Fluids*, **12** (1991) 655–82.
18. Hakonson, T., Bostick, K., Trujillo, G., Manies, K., Warren, R., Lane, L., Kent, J. & Wilson, W., Hydrologic Evaluation of Four Landfill Cover Designs at Hill Air Force Base, Utah. Los Alamos National Laboratory Report LA-UR-93-4469, Los Alamos, 1993.
19. Hills, R. G., Porro, I., Hudson, D. & Wierenga, P., Modeling of one dimensional infiltration into very dry soils 1. Model development and evaluation. *Water Resour. Res.*, **25** (1989) 1259–69.
20. Huyakorn, P. S. & Pinder, G. F., *Computational Methods in Subsurface Flow*. Academic Press NY, 1983.
21. Huyakorn, P., Thompson, S. & Thompson, B., Techniques for making finite element methods competitive in modelling flow in variably saturated porous media. *Water Resour. Res.*, **20** (1984) 1099–1115.
22. Huyakorn, P., Wu, Y. S., Panday, S., Park, N. S. & Forsyth, P. A., *MAGNAS User's Guide*, HydroGeoLogic Inc., NY, 1993.
23. Kirkland, M. R., Hills, R. G. & Wieranga, P. J., Algorithms for solving Richards' equation for variably saturated soils. *Water Resour. Res.*, **28** (1992) 2049–58.
24. Kool, J. & van Genuchten, M. Th., HYDRUS. A One Dimensional Variably Saturated Flow and Transport Model, Including Hysteresis and Root Water Uptake Version 3.3. US Salinity Laboratory Technical Report, US Department of Agriculture, Riverside, CA, USA, 1991.
25. Kool, J. B. & Wu, Y. S., Groundwater Flow and Transport Modelling of the NRC-licensed Waste Disposal Facility, West Valley, New York. US Nuclear Regulatory Commission Report NUREG/CR-5794 RW, NY, USA, 1991.
26. Kropinski, M. C., Numerical Techniques for Saturated–Unsaturated Flow. MSc., University of Waterloo, Dept. of Applied Mathematics, Canada, 1990.
27. Letniowski, F. W. & Forsyth, P. A., A control volume finite element method for three dimensional NAPL groundwater contamination. *Int. J. Num. Meth. Fluids*, **13** (1991) 955–70.
28. Li, C. W., A simplified Newton method with linear finite elements for transient unsaturated flow. *Water Resour. Res.*, **29** (1993) 965–71.
29. Meyer, P. D., Application of an Infiltration Evaluation Methodology to a Hypothetical Low-Level Waste Disposal Facility. US Nuclear Regulatory Commission Report NUREG/CR-6114, PNL-8842, NY, USA, 1993.
30. Ross, P. J., Efficient numerical methods for infiltration using Richards' equation. *Water Resour. Res.*, **26** (1990) 279–90.
31. Rubin, B. & Sammon, P. H., Practical control of timestep selection in thermal simulation. *SPE Reservoir Simulation Symposium*, 1983.
32. Sammon, P. H., An analysis of upstream weighting. *Soc. Pet. Eng. J. Res. Eng.*, **3** (1988) 1053–56.
33. Sleep, B. E. & Sykes, J. F., Compositional simulation of groundwater contamination by organic compounds 1. Model development and verification. *Water Resour. Res.*, **29** (1993) 1697–1708.
34. van der Vorst, H. A., Bi-CGSTAB: A fast and smoothly converging variant of Bi-CG for the solution of nonsymmetric linear systems. *SIAM J. Sci. Stat. Comp.*, **13** (1992) 631–45.
35. van Genuchten, M. Th., A closed form equation for predicting the hydraulic conductivity of unsaturated soils. *Soil Sc. Soc. Am. J.*, **44** (1980) 892–8.
36. Wu, Y. S., Kool, J. & McCord, J., *An Evaluation of Alternative Numerical Formulations for Two-Phase Air Water Flow in Unsaturated Soils*. AGU Spring meeting, Montreal, 1992.
37. Yeh, T.-C., Guxman, A., Srivastava, R. & Gagnard, P. E., Numerical simulation of the wicking effect in linear systems. *Groundwater*, **32** (1994) 2–11.
38. Zaidel, J. & Russo, D., Estimation of finite different interblock conductivities for simulation of infiltration into initially dry soils. *Water Resour. Res.*, **28** (1992) 2285–95.